

Polyalkynes Capped by Sulfur and Selenium

Daniel B. Werz and Rolf Gleiter*

Organisch-Chemisches Institut der Universität Heidelberg, Im Neuenheimer Feld 270,
D-69120 Heidelberg, Germany

rolf.gleiter@urz.uni-heidelberg.de

Received August 20, 2003

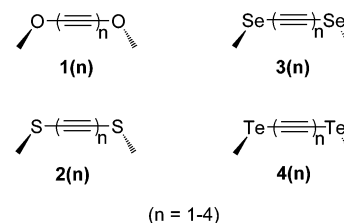
The synthesis of sulfur- and selenium-capped polyalkynes with two to four triple bonds was achieved. As starting materials the bis(trimethylsilyl)-protected polyalkynes were used, which were treated with MeLi/LiBr. The reaction of the resulting lithium salts with thiocyanatomethane and selenium/methyl iodide afforded **2(n)** and **3(n)**, respectively. Spectroscopic (PE and UV) and quantum chemical investigations show significant interaction between the chalcogen atoms. The structure of **3(4)** was investigated in the solid state, showing relatively short intermolecular Se...Se interactions.

Introduction

Carbon-rich rodlike molecules have attracted increasing attention from several points of view.¹ Unsaturated carbon chains have been used to link redox-active centers.² In many of these systems a significant interaction between terminal groups has been revealed by electrochemical data.² However, the rod itself also has been a center of interest: long, wire-like chains are considered as a model for the carbon allotrope “carbyne”.³ In all cases the termini play a crucial role. Usually bulky end groups were used to stabilize the highly unsaturated compounds.⁴ Systems with smaller endgroups are generally less stable and often explosive. Especially, examples with electron-rich main group elements as capping groups are rare.^{5–7} Recently, we studied the synthesis and the electronic and structural properties of tellurium-capped carbon rods **4(n)**.⁷ In seeking to extend this research, we

required access to lighter and more electron-rich chalcogens such as sulfur and selenium as substituents on the polyalkyne system.

CHART 1



Results and Discussion

The syntheses of **2(n)**, **3(n)** (Chart 1), and **5** were all carried out following the same pattern. We commenced with the corresponding alkyne **6(n)**,^{1b,8} protected with trimethylsilyl groups at both ends. From that we generated the bis(lithium) salts **7(n)** in situ by treating **6(n)** with methylolithium in the presence of lithium bromide at -78 to -30 °C. Subsequently thiocyanatomethane was added to obtain **2(n)** (Scheme 1). Similar procedures to place sulfur next to a triple bond were published previously.^{9,10} In the case of **2(2)** we also obtained the mono-(trimethylsilyl)-protected mono(methylthio)-substituted diyne **9**. In the synthesis of **3(n)** the bis(lithium) salt **7(n)** was treated at room temperature with powdered gray selenium to yield a highly nucleophilic diselenide **8(n)**, followed by capture by methyl iodide to afford **3(n)**. To reach **5** the intermediate **7(2)** was treated with phenylselenocyanate. With exception of **3(4)** all new species were

* To whom correspondence should be addressed. Fax: int-6221-544205.

(1) (a) Bohlmann, F. *Angew. Chem.* **1955**, *67*, 389–394. (b) Rubin, Y.; Lin, S. S.; Knobler, C. B.; Anthony, J.; Boldi, A. M.; Diederich, F. *J. Am. Chem. Soc.* **1991**, *113*, 6943–6949. (c) Schermann, G.; Grösser, T.; Hampel, F.; Hirsch, A. *Chem. Eur. J.* **1997**, *3*, 1105–1112. (d) Eisler, S.; Chahal, N.; McDonald, R.; Tykwinski, R. R. *Chem. Eur. J.* **2003**, *9*, 2542–2550.

(2) (a) Bruce, M. I.; Ke, M.; Low, P. J. *J. Chem. Soc., Chem. Commun.* **1996**, 2405–2406. (b) Bruce, M. I.; Ke, M. K.; Low, P. J.; Skelton, B. W.; White, A. H. *Organometallics* **1998**, *17*, 3539–3549. (c) Dembinski, R.; Bartik, T.; Bartik, B.; Jaeger, M.; Gladysz, J. A. *J. Am. Chem. Soc.* **2000**, *122*, 810–822. (d) Meyer, W. E.; Amoroso, A. J.; Horn, C. R.; Jaeger, M.; Gladysz, J. A. *Organometallics* **2001**, *20*, 1115–1127. (e) Coat, F.; Lapinte, C. *Organometallics* **1996**, *15*, 477–479. (f) Akita, M.; Chung, M.-C.; Sakurai, A.; Sugimoto, S.; Terada, M.; Tanaka, M.; Moro-oka, Y. *Organometallics* **1997**, *16*, 4882–4888. (g) Yam, V. W.-W.; Wong, K. M.-C.; Zhu, N. *Angew. Chem.* **2003**, *115*, 1438–1441; *Angew. Chem., Int. Ed.* **2003**, *42*, 1400–1403.

(3) Diederich, F.; Rubin, Y. *Angew. Chem.* **1992**, *104*, 1123–1126; *Angew. Chem., Int. Ed. Engl.* **1992**, *31*, 1101–1123.

(4) (a) Eastmond, R.; Johnson, T. R.; Walton, D. R. M. *Tetrahedron* **1972**, *28*, 4601–4616. (b) Jones, E. R. H.; Lee, H. H.; Whiting, M. C. *J. Chem. Soc.* **1960**, 3483–3489. (c) Gibtner, T.; Hampel, F.; Gisselbrecht, J.-P.; Hirsch, A. *Chem. Eur. J.* **2002**, *8*, 408–432 and references therein.

(5) Faul, D.; Himbert, G. *Chem. Ber.* **1988**, *121*, 1367–1369.

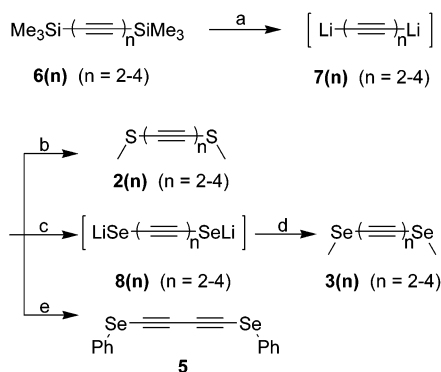
(6) (a) Gao, K.; Goroff, N. S. *J. Am. Chem. Soc.* **2000**, *122*, 9320–9321. (b) Hlavatý, J.; Kavan, L.; Štícha, M. *J. Chem. Soc., Perkin Trans. I* **2002**, 705–706.

(7) (a) Werz, D. B.; Gleiter, R.; Rominger, F. *Organometallics* **2003**, *22*, 843–849. (b) Gleiter, R.; Werz, D. B.; Rausch, B. *J. Chem. Eur. J.* **2003**, *9*, 2676–2683. (c) Werz, D. B.; Gleiter, R.; Rominger, F. *J. Am. Chem. Soc.* **2002**, *124*, 10638–10639.

(8) Walton, D. R. M.; Waugh, F. *J. Organomet. Chem.* **1972**, *37*, 45–56.

(9) Brandsma, L. *Preparative Acetylenic Chemistry*, 2nd ed.; Elsevier: Amsterdam, 1988.

(10) Benisch, C.; Bethke, S.; Gleiter, R.; Oeser, T.; Pritzkow, H.; Rominger, F. *Eur. J. Org. Chem.* **2000**, 2479–2488.

SCHEME 1^a

^a (a) MeLi/LiBr, THF, -78 to -30 °C; (b) MeSCN, THF, -30 °C; (c) Se, THF, rt; (d) MeI, THF, 0 °C; (e) PhSeCN, THF, -40 to 0 °C.

TABLE 1. Calculated Barriers of Rotation [kJ/mol] of **1(n) to **4(n)** for $n = 1-4$**

	$n = 1$	$n = 2$	$n = 3$	$n = 4$
1(n)	7.8	3.3	1.9	1.2
2(n)	19.7	10.6	6.6	4.2
3(n)	14.4	8.0	5.0	3.2
4(n)	11.5	6.9	4.3	2.8

yellow- to brown-colored oils that were purified by column chromatography. All of the alkynes with more than two triple bonds tend to polymerize after several weeks, even in the refrigerator. To derive the rotational energies of the methyl groups around the X-(CC)_n-X axis we have varied the torsional angle between the methyl groups from 90° (*C*₂) to 180° (*C*_{2h}) by using the DFT(B3LYP) method¹¹ applying a 6-311G(d) basis set.¹² The computations were carried out with the Gaussian98 program¹³ by optimizing all geometrical parameters. Frequency calculations were performed to characterize the nature of the stationary points. The results are summarized in Table 1. In all cases the preferred conformations reveal torsional angles (Me-X···X-Me) that are close to 90°. In all four acetylene derivatives we find the highest rotational energies for the sulfur-containing compounds **2(n)**, followed by the selenium, **3(n)**, tellurium, **4(n)**, and oxygen, **1(n)**, congeners. In comparison with hydrocarbon derivatives the calculated rotational barriers are remarkably high. Furthermore, we notice that the rotational barrier decreases with increasing *n*. A natural bond

(11) (a) Parr, R. G.; Yang, W. *Density-Functional Theory of Atoms and Molecules*; Oxford University Press: Oxford, 1989. (b) Koch, W.; Holthausen, M. C. *A Chemist's Guide to Density Functional Theory*; Wiley-VCH: Weinheim, 2000.

(12) Krishnan, R.; Binkley, J. S.; Seeger, R.; Pople, J. *J. Chem. Phys.* **1980**, *72*, 650–654.

(13) Frisch, M. J.; Trucks, G. W.; Schlegel, H. B.; Scuseria, G. E.; Robb, M. A.; Cheeseman, J. R.; Zakrzewski, V. G.; Montgomery, J. A., Jr.; Stratmann, R. E.; Burant, J. C.; Dapprich, S.; Millam, J. M.; Daniels, A. D.; Kudin, K. N.; Strain, M. C.; Farkas, O.; Tomasi, J.; Barone, V.; Cossi, M.; Cammi, R.; Mennucci, B.; Pomelli, C.; Adamo, C.; Clifford, S.; Ochterski, J.; Petersson, G. A.; Ayala, P. Y.; Cui, Q.; Morokuma, K.; Malick, D. K.; Rabuck, A. D.; Raghavachari, K.; Foresman, J. B.; Cioslowski, J.; Ortiz, J. V.; Baboul, A. G.; Stefanov, B. B.; Liu, G.; Liashenko, A.; Piskorz, P.; Komaromi, I.; Gomperts, R.; Martin, R. L.; Fox, D. J.; Keith, T.; Al-Laham, M. A.; Peng, C. Y.; Nanayakkara, A.; Gonzalez, C.; Challacombe, M.; Gill, P. M. W.; Johnson, B.; Chen, W.; Wong, M. W.; Andres, J. L.; Gonzalez, C.; Head-Gordon, M.; Replogle, E. S.; Pople, J. A. *Gaussian 98*, revision A.7; Gaussian, Inc.: Pittsburgh, PA, 1998.

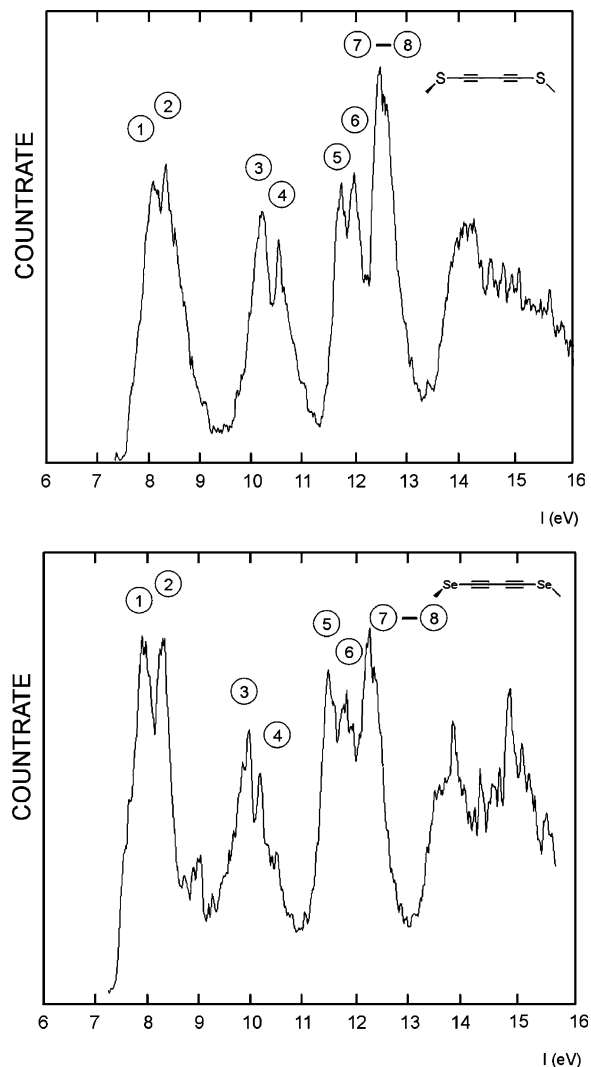


FIGURE 1. He(I) photoelectron spectra of **2(2)** (top) and **3(2)** (bottom).

orbital (NBO) analysis reveals that the magnitude of the rotational barriers results essentially as a compromise of two effects: the overlap between the lone pairs at the chalcogen atoms and the π^* orbitals and the energy difference between these orbitals. The overlap decreases from oxygen to tellurium. The same holds for the energy difference: it is largest for oxygen and smallest for tellurium. As a result the highest barriers for **2(n)** emerge.

To study the electronic structure further we recorded the He(I) and He(II) photoelectron spectra of **2(2)** and **3(2)**. In Figure 1 we show the He(I) spectra of **2(2)** and **3(2)**, which are very similar to each other. In Table 2 the first ionization energies of both species are collected. The PE spectra consist of four groups of close lying peaks to which we assign eight bands (see Figure 1). To each band we appoint a single ionization event due to the observation that the areas below the bands are very similar (see Table 2).

A comparison between the intensities of the He(I) and He(II) spectra shows almost no variations of the intensities for **2(2)** and only slight variations for **3(2)**. In the latter case we observe an increase for bands 1 and 2 and a decrease for bands 5–8 in the He(I) spectra. To

TABLE 2. Listing of Vertical Ionization Energies, $I_{v,j}$, Calculated Orbital Energies, ϵ_j , Assignments, and Relative Band Intensities from He(I) and He(II) PE Spectra of **2(2)** (top) and **3(2)** (bottom)

band	$I_{v,j}^a$	assignment ^b	$-\epsilon_j^a$	relative He(I)	relative He(II)
Data for 2(2)					
1	8.1	18b [n(p), π]	8.56	1.3 ^c	1.3 ^c
2	8.4	19a [n(p), π]	8.58		
3	10.2	18a [π]	11.15	1.0 ^c	1.0 ^c
4	10.5	17b [π]	11.16		
5	11.7	16b [π]	13.14	0.8 ^c	0.8 ^c
6	12.0	17a [π]	13.15		
7	12.5	16a [n(sp ⁿ), π]	14.06	1.0 ^c	0.9 ^c
8	12.6	15b [n(sp ⁿ), π]	14.07		
Data for 3(2)					
1	8.0	27b [n(p), π]	8.42	1.5 ^c	1.3 ^c
2	8.4	28a [n(p), π]	8.42		
3	9.9	27a [π]	10.67	1.0 ^c	1.0 ^c
4	10.2	26b [π]	10.68		
5	11.4	26a [π]	12.59	0.9 ^c	1.3 ^c
6	11.8	25b [π]	12.59		
7	12.2	25a [π , n(sp ⁿ)]	13.69	0.9 ^c	1.0 ^c
8	12.3	24b [π , n(sp ⁿ)]	13.70		

^a The ionization energies and orbital energies are given in eV.

^b The assignment of the bands to MOs is based on the assumption of C_2 symmetry. The numbering refers to the results of the HF calculation based on the geometry of lowest energy. ^c Average value, setting the intensity of the second peak to 1.0.

interpret these data we make use of empirical correlations between the PE data of **2(2)** and **3(2)** with those of **2(1)** and **3(1)**,¹⁴ respectively. We furthermore make use of the fact that the intensity of a PE band depends on the photon wavelength.¹⁵ As a rule He(I) photons favor the ejection of electrons from diffuse (delocalized) orbitals, whereas He(II) photons favor the ejection from contracted (localized) orbitals.¹⁵ We also rely on the validity of Koopmans' theorem, which assumes that the calculated orbital energy ($-\epsilon_j$) can be set equal to the vertical ionization energy ($I_{v,j}$) of the ionization event.¹⁶ In Figure 2 we show a correlation of **2(1)** with **2(2)** and **3(1)** with **3(2)**. This comparison suggests to assign the first two PE bands in **2(2)** and **3(2)** to ionization events from p-type lone pairs on the chalcogen centers.

Bands 3–6 are assigned to π orbitals that are mainly localized on the 1,3-butadiyne unit. Bands 7 and 8 are assigned to orbitals with large coefficients at the chalcogen centers (n-type). The He(II) data for **3(2)** are in line with this qualitative assignment. The strong mixing of p, n, and π basis orbitals is seen when one compares the centers of gravity of the “ π bands” 3 and 4 and those of 4 and 5. The energy difference between these centers is about 1.5 eV. This is considerably less than the energy difference found for the π bands in 1,3-butadiyne (2.5 eV).¹⁷ The assignment resulting from the empirical correlations are in line with the calculated orbital sequence. These calculations show that all frontier molecular orbitals are rather strongly delocalized. This

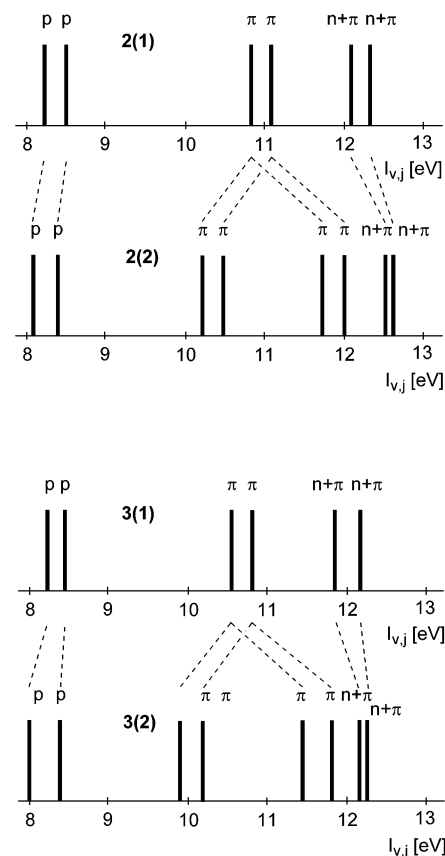


FIGURE 2. Correlation between the first PE bands of **2(1)** and **2(2)** (top) and **3(1)** and **3(2)** (bottom).

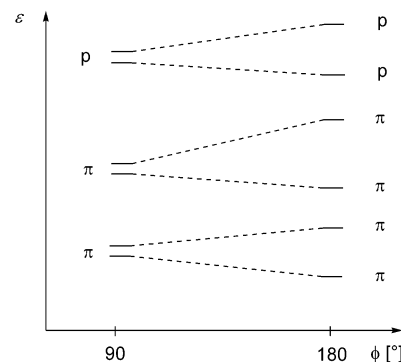


FIGURE 3. Qualitative correlation diagram between the highest occupied molecular orbitals for the torsional angle ϕ between the methyl groups.

rationalizes the small differences between the intensities of the He(I) and He(II) spectra of **2(2)** and **3(2)**.

In Figure 3 we have correlated the highest occupied molecular orbitals of **2(2)** for a torsion angle ϕ between the methyl groups of 90° and 180°. It is seen that for the perpendicular conformation bands 1–2, 3–4, and 5–6 form pairs. This mirrors the sequence of the first PE bands very well. Thus, this comparison suggests that the preferred conformation of **2(2)** in the gas phase is perpendicular.

The electronic absorption spectra of **2(2)** are compared with those of the congeners **2(1)**, **2(3)**, and **2(4)** in Figure 4. There, we present also the electronic spectra of **3(1)**, **3(2)**, **3(3)**, and **5**. This comparison reveals that the bands

(14) Bock, H.; Ried, W.; Stein, U. *Chem. Ber.* **1981**, *114*, 673–683.

(15) Price, W. C.; Potts, A. W.; Streets, D. G. In *Electron Spectroscopy*; Shirley, A. D., Ed.; North-Holland Publishing Company: Amsterdam, 1972; pp 187–198.

(16) Koopmans, T. *Physica* **1934**, *1*, 104–113.

(17) Turner, D. W.; Baker, C.; Baker, A. D.; Brundle, C. R. *Molecular Photoelectron Spectroscopy*; Wiley-Interscience: New York, 1970; pp 170–172.

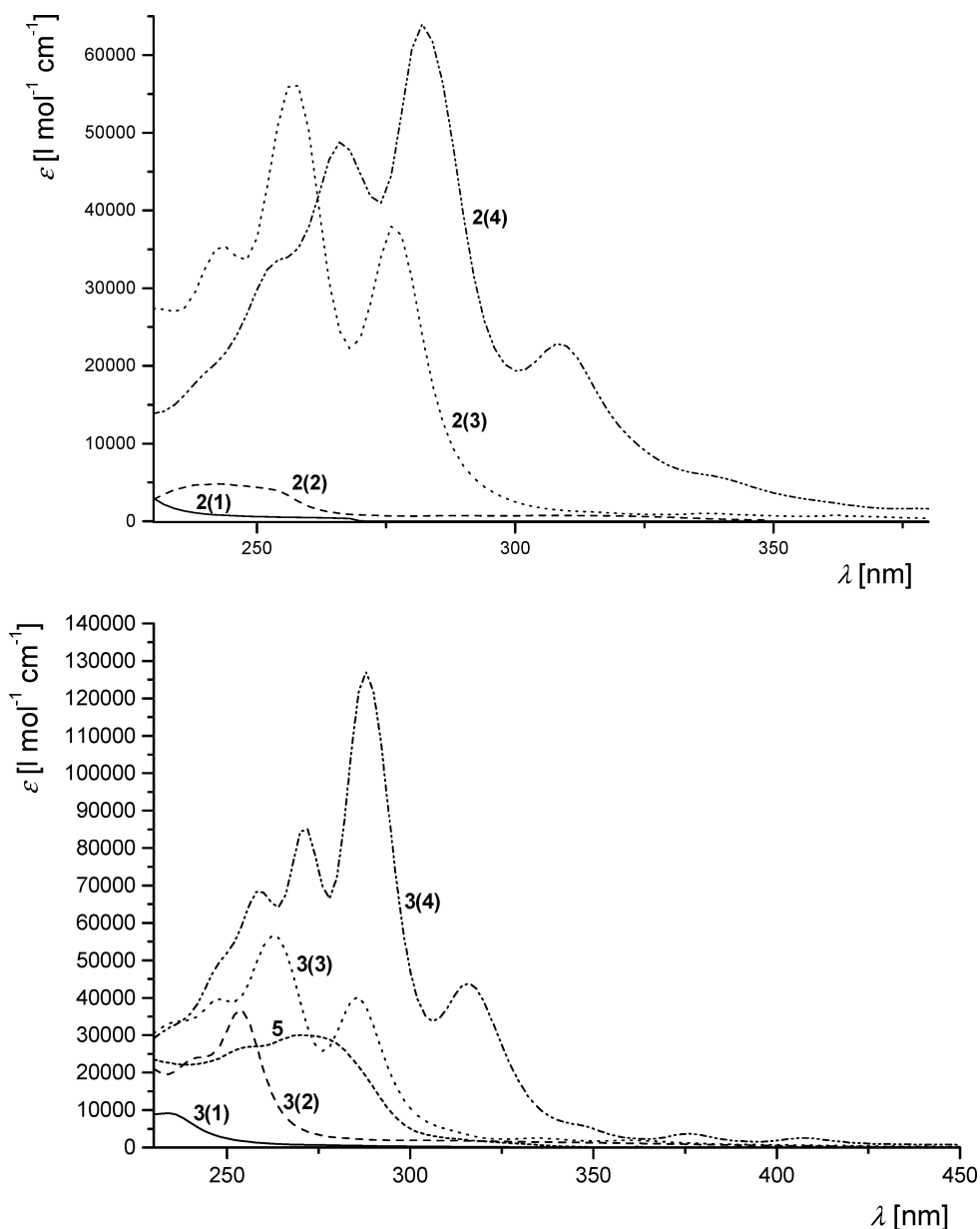


FIGURE 4. Electronic absorption spectra of **2(n)** ($n = 1-4$) (top) and **3(n)** ($n = 1-4$) as well as **5** (bottom).

at long wavelengths have lower intensity than those at shorter wavelengths. Investigations of the pure hydrocarbons revealed two types of bands: at shorter wavelengths the intense ${}^1\Sigma_g^+ \rightarrow {}^1\Sigma_u^+$ transition and at longer wavelengths the “forbidden” ${}^1\Sigma_g^+ \rightarrow {}^1\Delta_u$ transition of low intensity.^{18,19} The pattern found for the absorption spectra of **2(n)** and **3(n)** is also similar to that reported for various linear alkynes substituted with bulky groups at the termini²⁰ and with the tellurium congeners **4(n)**.⁷ As in the latter case we cannot exclude that the long wavelength bands of **2(n)** and **3(n)** might also arise from $n \rightarrow \pi^*$ transitions due to the lone pair character of the

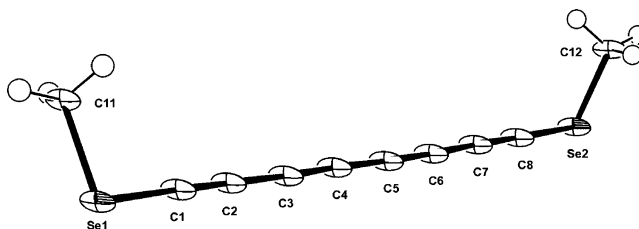


FIGURE 5. Molecular structure of **3(4)**.

HOMO. Figure 4 also shows that the $\pi \rightarrow \pi^*$ transition in **5** dominates the UV–vis spectrum.

Furthermore, we were able to elucidate the structure of **3(4)** in the solid state. In Figure 5 we show the molecular structure. Unfortunately, as a result of a fast decomposition process (the color of the crystals changed from deep yellow to black) the quality of the structure is mediocre ($R(F) = 0.099$), and therefore the data have to

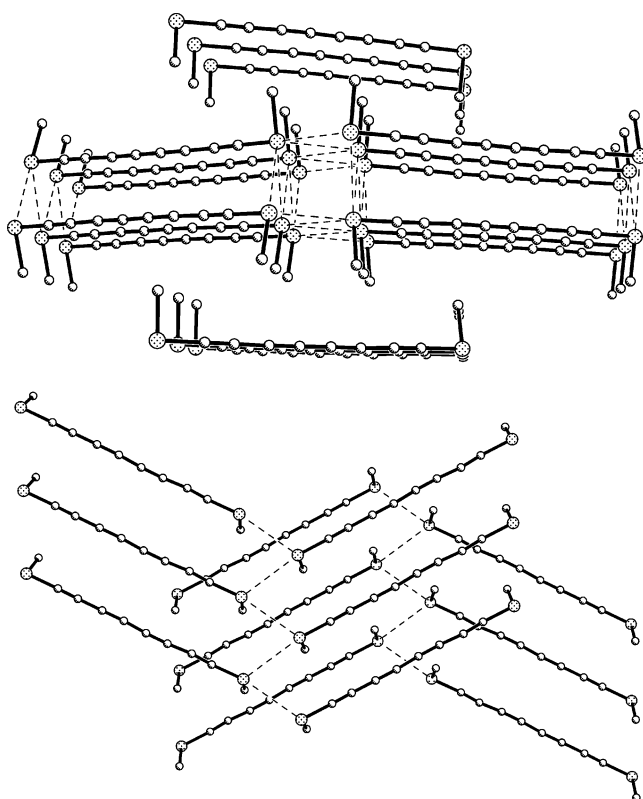
(18) Kloster-Jensen, E. *Angew. Chem.* **1972**, *84*, 483–485; *Angew. Chem., Int. Ed. Engl.* **1972**, *11*, 438–440.

(19) (a) Kloster-Jensen, E.; Haink, H.-J.; Christen, H. *Helv. Chim. Acta* **1974**, *57*, 1731–1744. (b) Haink, H.-J.; Jungen, M. *Chem. Phys. Lett.* **1979**, *61*, 319–322.

(20) Eastmond, R.; Walton, D. R. M. *Tetrahedron* **1972**, *28*, 4591–4599.

TABLE 3. Bond Lengths (Å), Bond Angles (deg), and Torsional Angles (deg) of 3(4)

Se1–C1	1.82(2)
Se1–C11	1.97(2)
Se2–C8	1.82(2)
Se2–C12	1.96(2)
C1–C2	1.17(2)
C2–C3	1.41(2)
C3–C4	1.25(2)
C4–C5	1.32(2)
C5–C6	1.24(2)
C6–C7	1.37(2)
C7–C8	1.19(2)
C1–Se1–C11	96(1)
C8–Se2–C12	98(1)
C2–C1–Se1	179(2)
C1–C2–C3	179(2)
C4–C3–C2	178(2)
C3–C4–C5	176(2)
C6–C5–C4	177(2)
C5–C6–C7	176(2)
C8–C7–C6	173(2)
C7–C8–Se2	176(2)
C11–Se1–Se2–C12	47(2)

**FIGURE 6.** Top view and side view of the structure of **3(4)** in the crystal. The short contacts between the Se centers are indicated.

be taken with a grain of salt. Nevertheless, we find a torsional angle of 47° between the terminal CH_3 groups and the anticipated bond alternation between the triple bonds. In Table 3 we have listed the most relevant bond distances and angles of **3(4)**. The structural parameters are close to those reported for **4(4)**.^{7a} More interesting is the arrangement of the rods in the solid state, which is shown in Figure 6. The molecules pile up on top of each other while the Se centers keep close contacts (between 3.67 and 3.73 Å), giving rise to a zigzag

arrangement. A similar structure was observed for the tellurium congener.^{7a}

In summary, we developed a convenient method to synthesize sulfur- and selenium-capped carbon rods by using the rather stable bis(trimethylsilyl)-protected polyalkynes as starting materials. Our spectroscopic investigations on **2(n)** and **3(n)** ($n = 1-4$) show that there is a considerably interaction between the lone pairs of the chalcogen centers. In the cases of **2(2)** and **3(2)** our PE studies reveal energy difference values between 0.3 and 0.4 eV. For **3(4)** we found strong intermolecular $\text{Se}\cdots\text{Se}$ interactions leading to the formation of stacks.

Experimental Section

General Procedure for Preparation of 2(n) and 9. To a solution of bis(trimethylsilyl)alkyne in 100 mL of THF was added MeLi/LiBr in diethyl ether (1.5 M) dropwise at -78°C over a period of 15 min. The solution was stirred for 3 h at -78°C . After that, the reaction mixture was allowed to warm slowly to -30°C . A solution of thiocyanatomethane in THF was added dropwise at -30°C . After completing the addition, the reaction mixture was stirred for 1 h while keeping the temperature below -10°C . Next, 50 mL of saturated NH_4Cl solution and 200 mL of hexane were added, the layers were separated, and the aqueous layer was extracted three times with diethyl ether, yielding a yellow solution. The organic layer was dried with anhydrous MgSO_4 . After removal of the solvent the crude product was absorbed on Celite. The product was purified by column chromatography {silica gel [3% NET_3 (v/v)], *n*-hexane}.

2,7-Dithioocta-3,5-diyne (2(2)) and (Trimethylsilyl)-(methylthio)butadiyne (9). Starting materials were 1.00 g (5.14 mmol) of 1,4-bis(trimethylsilyl)buta-1,3-diyne (**6(2)**), 7.9 mL (11.9 mmol) of MeLi/LiBr in diethyl ether, and 0.75 g (10.3 mmol) thiocyanatomethane. Column chromatography afforded 156 mg (21%) of **2(2)** and 252 mg (29%) of **9**. Analytical data of **2(2)**: yellow oil; ^1H NMR (CDCl_3 , 300 MHz) δ 2.41 (s, 6H, CH_3); ^{13}C NMR (CDCl_3 , 75 MHz) δ 19.4 (S CH_3), 75.2 (SCC), 79.8 (SCC); IR (film) 2926, 2117, 2077, 1428, 1309 cm^{-1} ; UV-vis (CH_2Cl_2) λ_{max} , nm (ϵ , $\text{M}^{-1}\text{cm}^{-1}$) 244 (74000), 290 (7300), 308 (7400); (EI, 70 eV) m/z 142 (M^+ , 100), 127 ($[\text{M} - \text{CH}_3]^+$, 76), 112 ($[\text{M} - 2\text{CH}_3]^+$, 93). HRMS (EI) calcd for $\text{C}_6\text{H}_6\text{S}_2$ 141.9912, found 141.9912. Anal. Calcd for $\text{C}_6\text{H}_6\text{S}_2$ (142.25): C, 50.66; H, 4.25; S, 45.09. Found: C, 50.58; H, 4.30; S, 45.22. Analytical data of **9**: yellow oil; ^1H NMR (CDCl_3 , 300 MHz) δ 0.19 (s, 9H, $\text{Si}(\text{CH}_3)_3$), 2.42 (s, 6H, CH_3); ^{13}C NMR (CDCl_3 , 75 MHz) δ 0.25 ($\text{Si}(\text{CH}_3)_3$), 18.8 (S CH_3), 71.2 (CC), 78.8 (CO), 88.3 (CC), 88.6 (CC); IR (film) 2960, 2930, 2899, 2267, 2163, 2076, 1421 cm^{-1} ; UV-vis (CH_2Cl_2) λ_{max} , nm (ϵ , $\text{M}^{-1}\text{cm}^{-1}$) 254 (4200), 268 (6100), 282 (6800), 300 (4200); (EI, 70 eV) m/z 168 (M^+ , 39), 153 ($[\text{M} - \text{CH}_3]^+$, 100), 138 ($[\text{M} - 2\text{CH}_3]^+$, 27). HRMS (EI) calcd for $\text{C}_8\text{H}_{12}\text{SSi}$ 168.0429, found 168.0415.

2,9-Dithiadeca-3,5,7-triyne (2(3)). Starting materials were 477 mg (2.04 mmol) of 1,6-bis(trimethylsilyl)hexa-1,3,5-triyne (**6(3)**), 3.2 mL (4.7 mmol) of MeLi/LiBr in diethyl ether (1.5 M), and 344 mg (4.7 mmol) of thiocyanatomethane. Column chromatography afforded 158 mg (46%) of **2(3)** as a dark yellow oil; ^1H NMR (CDCl_3 , 300 MHz) δ 2.43 (s, 6H, CH_3); ^{13}C NMR (CDCl_3 , 75 MHz) δ 19.1 (S CH_3), 65.9 (SCCO), 74.1 (SC), 79.9 (SCC); IR (film) 2927, 2233, 2134, 1429, 1312 cm^{-1} ; UV-vis (CH_2Cl_2) λ_{max} , nm (ϵ , $\text{M}^{-1}\text{cm}^{-1}$) 244 (35300), 258 (56100), 276 (37600), 314 (1000), 338 (1000), 364 (700), 394 (300); (EI, 70 eV) m/z 166 (M^+ , 94), 151 ($[\text{M} - \text{CH}_3]^+$, 53), 136 ($[\text{M} - 2\text{CH}_3]^+$, 100). HRMS (EI) calcd for $\text{C}_8\text{H}_6\text{S}_2$ 165.9911, found 165.9895.

2,11-Dithiadodeca-3,5,7,9-tetrayne (2(4)). Starting materials were 380 mg (1.57 mmol) of 1,8-bis(trimethylsilyl)octa-1,3,5,7-tetrayne (**6(4)**), 2.4 mL (3.61 mmol) of MeLi/LiBr in diethyl ether, and 264 mg (3.61 mmol) of thiocyanatomethane. Column chromatography afforded 58 mg (20%) of **2(4)** as a brown oil; ^1H NMR (CDCl_3 , 500 MHz) δ 2.45 (s, 6H, CH_3); ^{13}C

NMR (CDCl₃, 125 MHz) δ 19.0 (SCH₃), 64.5 (C), 66.3 (C), 73.7 (S C), 80.0 (S C); IR (film) 2957, 2928, 2164, 2045, 1429, 1311, 1248 cm⁻¹; UV-vis (CH₂Cl₂) λ_{\max} , nm (ϵ , M⁻¹ cm⁻¹) 254 (33600), 266 (48600), 282 (63800), 308 (22800), 332 (6600), 374 (1000), 410 (1900); (EI, 70 eV) m/z 190 (M⁺, 78), 175 ([M - CH₃]⁺, 46), 160 ([M - 2CH₃]⁺, 100). HRMS (EI) calcd for C₁₀H₆Se₂ 189.9911, found 189.9890.

General Procedure for Preparation of 3(n). To a solution of bis(trimethylsilyl)alkyne in 100 mL of THF was added MeLi/LiBr in diethyl ether (1.5 M) dropwise at -78 °C over a period of 15 min. The solution was stirred for 3 h at -78 °C. After that, the reaction mixture was allowed to warm slowly to room temperature. The powdered gray selenium was added in one portion. The reaction mixture was stirred for 1 h and then was cooled to 0 °C. A solution of methyl iodide in THF was added over a period of 10 min. After the addition was complete the stirring was continued for 1 h at 0 °C. The workup and column chromatography followed as described for 2(n).

2,7-Diselenaocta-3,5-diyne (3(2)). Starting materials: 1.00 g (5.14 mmol) of 1,4-bis(trimethylsilyl)buta-1,3-diyne (**6(2)**), 7.9 mL (11.9 mmol) of MeLi/LiBr in diethyl ether, 0.94 g (10.3 mmol) of powdered gray selenium and 1.68 g (11.9 mmol) of methyl iodide. Column chromatography afforded 530 mg (44%) of **3(2)** as a brown oil: ¹H NMR (CDCl₃, 300 MHz) δ 2.33 (s, 6H, CH₃); ¹³C NMR (CDCl₃, 75 MHz) δ 9.9 (SeCH₃), 75.2 (SeCC), 79.8 (SeCC); IR (film) 2930, 2119, 2065, 1762, 1417 cm⁻¹; UV-vis (CH₂Cl₂) λ_{\max} , nm (ϵ , M⁻¹ cm⁻¹) 240 (24100), 254 (36900), 282 (2600), 300 (1900); (EI, 70 eV) m/z 238 (M⁺, 100), 223 ([M - CH₃]⁺, 58), 208 ([M - 2CH₃]⁺, 78). HRMS (EI) calcd for C₆H₆Se₂ 237.8800, found 237.8799. Anal. Calcd for C₆H₆Se₂ (236.0): C, 30.53; H, 2.56. Found: C, 30.68; H, 2.69.

2,9-Diselena-deca-3,5,7-triyne (3(3)). Starting materials were 1.35 g (6.21 mmol) of 1,6-bis(trimethylsilyl)hexa-1,3,5-triyne (**6(3)**), 9.5 mL (14.3 mmol) of MeLi/LiBr in diethyl ether (1.5 M), 1.13 g (14.3 mmol) of powdered gray selenium, and 2.03 g (14.3 mmol) methyl iodide. Column chromatography afforded 484 mg (30%) of **3(3)** as a brown oil: ¹H NMR (CDCl₃, 300 MHz) δ 2.40 (s, 6H, CH₃); ¹³C NMR (CDCl₃, 75 MHz) δ 9.8 (SeCH₃), 64.4 (SeCC), 65.9 (SeC), 85.2 (SeCC); IR (film) 2932, 2151, 1420, 1269 cm⁻¹; UV-vis (CH₂Cl₂) λ_{\max} , nm (ϵ , M⁻¹ cm⁻¹) 238 (33800), 248 (39700), 262 (56400), 286 (40000), 334 (2400), 358 (1900); (EI, 70 eV) m/z 262 (M⁺, 100), 247 ([M - CH₃]⁺, 52), 232 ([M - 2CH₃]⁺, 100). HRMS (EI) calcd for C₈H₆Se₂ 261.8800, found 261.8799.

2,11-Diselena-deca-3,5,7,9-tetrayne (3(4)). Starting materials were 293 mg (1.21 mmol) of 1,8-bis(trimethylsilyl)octa-1,3,5,7-tetrayne (**6(4)**), 2.1 mL (3.1 mmol) of MeLi/LiBr in diethyl ether (1.5 M), 275 mg (3.5 mmol) of powdered gray selenium, and 475 mg (3.3 mmol) methyl iodide. Column chromatography afforded 82 mg (24%) of **3(4)** as a deep yellow

solid: mp 63 °C; ¹H NMR (CDCl₃, 500 MHz) δ 2.37 (s, 6H, CH₃); ¹³C NMR (CDCl₃, 125 MHz) δ 9.8 (SeCH₃), 63.9 (C), 64.9 (C), 66.1 (C), 85.5 (C); IR (film) 2934, 2168, 2039, 1656, 1633, 1414, 1260 cm⁻¹; UV-vis (CH₂Cl₂) λ_{\max} , nm (ϵ , M⁻¹ cm⁻¹) 250 (52000), 258 (68300), 272 (85100), 288 (127000), 316 (44000), 346 (6100), 376 (3400), 408 (2300); (EI, 70 eV) m/z 286 (M⁺, 100), 271 ([M - CH₃]⁺, 45), 256 ([M - 2CH₃]⁺, 97). HRMS (EI) calcd for C₁₀H₆Se₂ 285.8800, found 285.8792. Anal. Calcd for C₁₀H₆Se₂ (284.1): C, 42.28; H, 2.13. Found: C, 42.28; H, 2.73.²¹ Crystal data: dimensions 0.16 × 0.11 × 0.07 mm³, crystal system orthorhombic, space group *Pbcn*, *Z* = 8, *a* = 15.596(4) Å, *b* = 4.3034(11) Å, *c* = 28.359(7) Å, *V* = 1903.4(8) Å³, *D*_{calc} = 1.983 g/cm³, *T* = 100(2) K, θ_{\max} = 23.24°, 11002 reflections measured, 1370 unique, 738 observed, μ = 7.71 mm⁻¹, *T*_{min} = 0.37, *T*_{max} = 0.61, 45 parameters refined, *S*(Gof) = 1.02, *R*(F) = 0.099, *R*_w(F²) = 0.240, residual electron density -1.26 to 8.61 e Å⁻³.

Bis(phenylseleno)butadiyne (5). Instead of selenium powder and an alkylating reagent, phenylselenocyanate was used and was added dropwise at -40 °C into the reaction mixture. Starting materials were 1.00 g (5.14 mmol) of 1,4-bis(trimethylsilyl)buta-1,3-diyne, 7.9 mL (11.9 mmol) of MeLi/LiBr in diethyl ether (1.5 M), and 1.87 g (10.3 mmol) of phenylselenocyanate. Column chromatography afforded 979 mg (53%) of **5** as a brown oil: ¹H NMR (CDCl₃, 500 MHz) δ 7.35 (m, 6H, Ph*H*), 7.55 (m, 4H, Ph*H*); ¹³C NMR (CDCl₃, 125 MHz) δ 65.7 (SeCC), 89.4 (SeCC), 127.6 (SeC(Ph)), 127.9 (C(Ph)), 129.7 (C(Ph)), 129.8 (C(Ph)); IR (film) 3057, 2360, 2137, 2067, 1575, 1475 cm⁻¹; UV-vis (CH₂Cl₂) λ_{\max} , nm (ϵ , M⁻¹ cm⁻¹) 256 (25800), 270 (29000); (EI, 70 eV) m/z 362 (M⁺, 45), 281 (44), 202 (100). HRMS (EI) calcd for C₁₆H₁₀Se₂ 361.9113, found 361.9150. Anal. Calcd for C₁₆H₁₀Se₂ (360.2): C, 53.36; H, 2.80. Found: C, 53.51; H, 2.96.

Acknowledgment. We are grateful to the Deutsche Forschungsgemeinschaft, the Fonds der Chemischen Industrie and the BASF Aktiengesellschaft, Ludwigshafen, for financial support. D.B.W. thanks Jens Nägele for preparative assistance and the Studienstiftung des deutschen Volkes for a graduate fellowship.

Supporting Information Available: General experimental procedures. He(II) spectra of **2(2)** and **3(2)**. Cartesian coordinates, number of imaginary frequencies, and total energies of compounds **1(n)**, **2(n)** and **3(n)** in *C*₂ and *C*_{2h} symmetry. Crystal data for compound **3(4)**. This material is available free of charge via the Internet at <http://pubs.acs.org>.

JO0352171

(21) The decomposition that takes place is responsible for giving no satisfactory values for hydrogen in the combustion analysis.